Research article

Rhodamine 6G derivative for the selective copper detection and remediation using nanoporous diatomaceous earth-engineered functional receptor

Padmaja V. Mane [a,1], Pravin Patil [b,1], Anusha A. Mahishi [a], Madhuprasad Kigga [a], Mahesh P. Bhat [c,*], Kyeong-Hwan Lee [c,d,e,**], Mahaveer Kurkuri [a,***]

[a] Centre for Research in Functional Materials (CRFM), JAIN (Deemed-to-be University), Jain Global Campus, Bengaluru 562112, Karnataka, India
[b] Post-Graduate Department of Studies and Research in Chemistry, K. L. E. Society's, P. C. Jabin Science College, Vidyanagar 580031, Hubballi, Karnataka, India
[c] Agricultural Automation Research Centre, Chonnam National University, Gwangju 61186, South Korea
[d] Department of Convergence Biosystems Engineering, Chonnam National University, Gwangju 61186, Republic of Korea
[e] BK21 Interdisciplinary Program in IT-Bio Convergence System, Chonnam National University, Gwangju 61186, Republic of Korea

A B S T R A C T

A rhodamine-derived receptor was synthesized and comprehensively characterized for structural confirmation. The receptor was able to distinguish the copper ions (Cu^{2+}) from other competing cations. The yellow color of the receptor changed to pink upon adding Cu^{2+} ions, however, other competing cations ions were impotent towards any color variation. The UV–visible titration studies revealed the binding stoichiometry of a 1:1 ratio with a detection limit of 9.663×10^{-8} M. Additionally, a novel idea of the work resides in the use of diatom for the practical application, where the receptor has been tethered on nanoporous diatomaceous earth microparticles (P2D) to remove Cu^{2+} ions. The results confirmed that 50 mg receptor functionalized DE could adsorb 10 mL of 1 ppm Cu^{2+} ions from water. Furthermore, a proof-of-concept device that is inexpensive, simple to operate, and continuously removes Cu^{2+} ions from water has been developed. The efficiency of the device in Cu^{2+} ion removal could be realized through the naked eye by observing the color change of P2D particles, which has excellent potential for application in remote locations where water contamination is a significant issue.

1. Introduction

Copper is the third abundant metal present in living beings which plays a vital role in various metabolic activities of the human body. It has significance in a large number of redox and catalytic actions of various enzymes [1]. The healthy cells contain

* Corresponding author.
** Corresponding author. Agricultural Automation Research Centre, Chonnam National University, Gwangju 61186, South Korea
*** Corresponding author. Centre for Research in Functional Materials (CRFM), JAIN (Deemed-to-be University), Jain Global Campus, Bengaluru 562112, Karnataka, India
  E-mail addresses: mahesh1306@chonnam.ac.kr (M.P. Bhat), khlee@chonnam.ac.kr (K.-H. Lee), mahaveer.kurkuri@jainuniversity.ac.in (M. Kurkuri).
  [1] Padmaja V. Mane and Pravin Patil contributed equally.

approximately 100 mM of Cu^{2+} ions in their complex form [2]. However, the presence of free Cu^{2+} ions in living cells is extremely low i.e., one free ion per cell. It has been observed that excess consumption of Cu^{2+} can cause diseases related to neurodegenerative ailments including Alzheimer's disease [3], Wilsons disorder [4], amyotrophic lateral sclerosis (motor neuron disease) [5], Menkes syndrome [6], and Parkinson's disease [7]. Therefore, the US EPA (United States Environmental Protection Agency) has set a permissible limit of 1.3 ppm for Cu^{2+} ions in drinking water [8].

The Cu^{2+} ions were investigated systematically using a broad range of analytical techniques such as atomic absorption spectrometry (AAS) [9], atomic emission spectrometry (AES) [10], and inductively coupled plasma mass spectroscopy (ICP-MS) [11]; which has great sensitivity, selectivity, high efficiency, and reliability. However, all these methods are expensive, require advanced instrumentation, and skilled personnel to operate, which will be a setback to use these methods in field applications [12,13]. To overcome the above issues, a lot of effort has been put into the growth of new and more reliable approaches for the selective and sensitive recognition of Cu^{2+} ions. Among all explored methods, colorimetric detection drew a lot of attention because of their excellent practicality including the inexpensive, rapid response that could be seen through the naked eye, minimal usage of sophisticated instruments, and potential for the development of portable devices for use in field applications [14,15].

Owing to the above advantages, the design and introduction of advanced organic sensors that detect the Cu^{2+} ions are of considerable attention. Several organic sensors have been explored in the past few years for the recognition of Cu^{2+} ions. These efforts do, however, have certain drawbacks, including tedious synthetic procedures, cross-sensitivities in presence of several other cations, and the fact that these molecules were useful in solution form. Nevertheless, rhodamine derivatives have gained prominence due to their distinct optical characteristics, which include high absorption, emission wavelengths, and a high molar extinction coefficient. These molecules exhibit broad variations in absorbance/fluorescence intensities that induce a noticeable color change upon binding with Cu^{2+} ions, allowing 'naked eye' detection [16]. Apart from this, they can be easily modified and functionalized on solid substrates. As a result of these attributes, these are more appealing in the field of cation detection and removal as well.

In addition, due to the toxicity of organic receptors, functionalizing them on inorganic materials (solid substrates) is highly sought to prevent molecules from leaching into the water system. The choice of solid supports with eminent properties mainly large surface area, high porosity, and simpler functionalization are important to display remarkable high selectivity and sensitivity upon immobilizing organic receptors. So far, though various organic-inorganic hybrid materials reported in the literature including metal-oxide nanoparticles [17], polymers [18], graphene-based materials [19], etc, are highly sought, they still have limitations such as the use of toxic chemicals during preparation, high cost, and ease of availability. It is worth noting that, to date, only limited receptor-functionalized inorganic materials reported, have the potential for practical applications. Therefore, there is a lot of interest in structurally stable molecules that can detect and remediate Cu^{2+} ions from water with specificity.

As conventional synthetic materials have the aforementioned drawbacks, nature has created a diverse range of materials to overcome them. Among all, diatomaceous earth microparticles (diatoms/DE) are of high importance due to their large surface area, nano porosity, biocompatibility, chemical inertness, surface tunability, and lightweight because of their hollow structure. They are porous sedimentary rocks made up of the prehistoric remains of algae with microscopic, unicellular 3D structured shells of amorphous hydrated silica. Further, they have been used in various fields such as water purification [20], nanofabrication [21], drug delivery [22], catalysis [23], pest control [24], solar cells [25], and supercapacitors [26]. However, the immobilization of rhodamine derivative on diatoms for Cu^{2+} ion removal is not explored to date. It is also noted that in almost many reported works, they have only discussed about the detection of metal ions, but the molecule synthesized by our group is utilized for the simultaneous detection and remediation of copper. Hence the significance of our work mainly lies in the removal studies using a naturally available high surface area material (Diatom) that is prone to functionalization.

In our previous work, we reported the molecule (rhodamine-6G derivative, P2) for molecular logic gate applications [27]. However, we had not explored the potential of the P2 molecule for selective recognition and remediation applications. Thus, the present study is an extension experimentation using the same rhodamine-6G derivative (P2) bearing 2-hydroxy-5-nitro benzaldehyde for the specific detection and remediation of Cu^{2+} ions from water. P2 was characterized with certain analytical techniques such as ^{1}H-NMR, ^{13}C-NMR, FTIR, and HRMS for structural conformations. Further, P2 was been immobilized on diatoms (DE) which were confirmed by FESEM, EDAX, and BET analysis. In addition to this, a simple, affordable device has been designed to continuously remove Cu^{2+} ions from water samples which are of great interest for field applications.

2. Experimental section

2.1. Materials

Rhodamine-6G, 2-hydroxy-5-nitro Benzaldehyde, and 3-aminopropyl-triethoxy silane (APTES) were bought from Sigma-Aldrich (India). Diatomaceous earth (DE) was received from Mount Sylvia (Australia) Pvt. Ltd. Toluene and Dimethylformamide (DMF) were purchased from Spectrochem (India). All the metal nitrates were bought from NICE chemicals (India). Ethanol was received from Changshu Hong Sheng Fine Chemicals (China). The solution of all the metal ions was prepared using distilled water.

The prepared organic molecules (P1 and P2) were analyzed for structural confirmations using ^{1}H NMR (proton nuclear magnetic resonance) and ^{13}C NMR (carbon-13 nuclear magnetic resonance) by Bruker (500 MHz) instrument where tetramethylsilane (TMS) is used as a standard reference and DMSO-d_6 as a solvent. FTIR (Fourier-transform infrared spectroscopy) analysis was performed for structural and functional confirmations with a Perkin Elmer II spectrometer. HRMS (High-resolution mass spectrometry) data were acquired utilizing a Waters Synapt G2 high-resolution mass spectrometer to confirm the formation of the receptor. UV–vis spectroscopic studies were done using Shimadzu 1700 PC UV–visible spectrophotometer in a standard 10 mm cuvette to investigate the

interaction of Cu^{2+} ions with the receptor. The P2 functionalized diatoms (P2D) were analyzed using a FESEM (field emission scanning electron microscope) to evaluate the morphological changes; images were taken from the JEOL instrument (FESEM/JEOL/JSM-7100F), Singapore Inc. Elements in the synthesized material were analyzed by EDAX (energy dispersive X-ray spectroscopy) using a ThermoFisher Scientific Pvt. Ltd. Ultra-Dry EDS Detector. BET (Brunauer-Emmett-Teller) surface analysis was carried out using BELSORP Max., Microtrac BEL.

2.2. Synthesis of P1

An ethanolic solution of Rhodamine-6G (2.090 Mm, 5 mL) was treated with 6.26 Mm of hydrazine hydrate. The reaction mixture was sonicated for 10 min to obtain a pink-colored solid product (Scheme S1). The product formed was then filtered and rinsed with ethanol to remove any unreacted reactants present and was allowed to dry at 60 °C to yield P1 (428.53 g/mol). The yield obtained: 0.72 g, 80%; m.p.: 235 °C; $C_{26}H_{28}N_4O_2$ calculated: C, 72.86; H, 6.60; N, 13.10; found: C, 72.59; H, 6.82; N, 13.09%; FTIR: 600 to 1650 cm^{-1} (xanthene moiety), 2791 cm^{-1} (C–H stretching), and 3423 cm^{-1} (N–H stretching) (Fig. S1); ^{13}C NMR (DMSO- d_6, 100 MHz, δ/ppm): 165.7, 152.5, 147.9, 132.7, 130.0, 128.4, 127.5, 123.9, 122.6, 118.3, 105.5, 96.4, 65.5, 38.0, 17.5, 14.7. (Fig. S2); ^1H NMR (DMSO-d_6, 500 MHz, δ/ppm): 7.757 (1H, d, $J = 5$ Hz), 7.458 (2H, d, $J = 5$ Hz), 6.932 (1H, d, $J = 5$ Hz), 6.264 (2H, s), 6.096 (2H, s), 4.995 (2H, t, $J = 5$ Hz), 4.217 (1H, s), 3.127 (2H, m, $J = 5$ Hz), 1.855 (3H, s), 1.205 (3H, t, $J = 10$ Hz) (Fig. S3).

2.3. Synthesis of P2

Obtained P1 (0.50 g, 1.17 mM) was dispersed in 15 mL of ethanol and a drop of acetic acid was added to catalyze the reaction. Further, 2-hydroxy 5-nitro benzaldehyde (0.19 g, 1.17 mM) was introduced while vigorously swirling and refluxed at 80 °C for 6 h to obtain a pale orange-colored precipitate P2 (577.63 g/mol). The filtrate was washed with ethanol to clean the unreacted reactants which were further allowed to dry overnight at 60 °C (Scheme S1). The yield obtained: 0.62 g, 93%; m.p.: 144 °C; $C_{33}H_{31}N_5O_5$ calculated: C, 68.59; H, 5.39; N, 12.15; found: C, 68.62; H, 5.40; N, 12.21%. FTIR: 600 to 1650 cm^{-1} (xanthene moiety), 1386 cm^{-1} (NO_2 group), 1466 cm^{-1} (C–H bending), 1628 cm^{-1} (C=C stretching), 2782 cm^{-1} (C–H stretching), and 3437 cm^{-1} (N–H stretching) (Fig. S4). ^{13}C NMR (DMSO- d_6, 400 MHz): 164.3, 162.6, 152.0, 151.4, 148.3, 143.3, 140.4, 134.6, 129.3, 128.5, 127.1, 127.0, 124.2, 123.6, 123.4, 120.8, 118.8, 117.5, 104.7, 96.2, 66.0, 38.0, 17.4, 14.6 (Fig. S5); ^1H NMR (DMSO-d_6, 500 MHz, δ/ppm): 12.084 (1H, s), 8.760 (1H, s), 8.030 (1H, d, $J = 8.8$ Hz), 7.964 (1H, d, $J = 7.2$ Hz), 7.541 (2H, q, $J = 7.6$ Hz), 6.912 (1H, d, $J = 7.2$ Hz), 6.443 (2H, s), 6.272 (2H, s), 3.537 (2H, s), 3.217 (4H, q), 1.880 (6H, s), 1.310 (6H, s) (Fig. S6); HRMS $[M]^+$: 577.2325, $[M+H]^+$: 578.2545 (Fig. S7).

2.4. Synthesis of P2D

P2D synthesis was carried out according to our earlier report with modifications [28]. The prepared 0.20 g of P2 was treated with
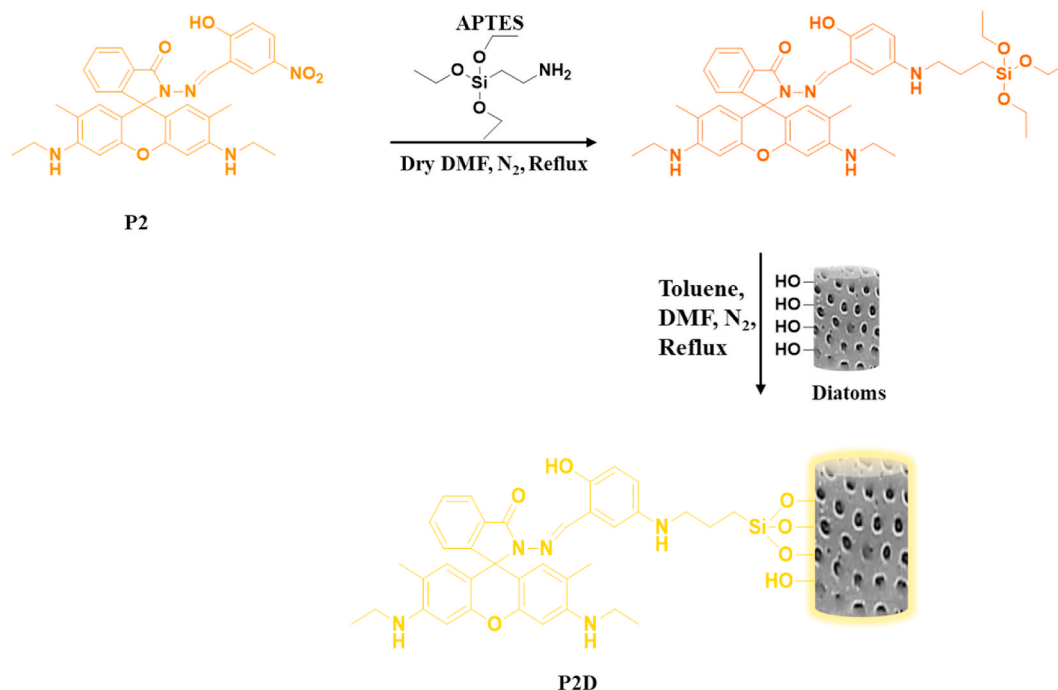
Scheme 1. Synthesis mechanism of P2D.

APTES (38 mg, 0.172 mmol) and dispersed in 5 mL of anhydrous DMF. Under the N_2 environment, the reaction mixture was stirred at 60 °C for 3 h. This results in the reaction between the $-NO_2$ group of P2 and the $-NH_2$ group of APTES to form an intermediate [29]. Further, nanoporous diatomaceous earth microparticles dispersed in 20 mL of toluene were added to the above product and refluxed for 24 h at 110 °C under N_2 atmosphere. As the reaction was completed, the formed final product was centrifuged, washed with methanol to remove unreacted reactants and initial solvents, and dried under vacuum conditions at 60 °C. Hereafter this material is coded as P2D (Scheme 1). Further FTIR analysis was performed to identify the formation of P2D: 1000 to 1690 cm^{-1} (xanthene moiety), 1694 cm^{-1} (C=O stretching), and 3612 cm^{-1} (N–H stretching) (Fig. S8).

3. Results and discussion

3.1. Naked eye detection of Cu^{2+} ions

To evaluate the cation-induced color change, a 2 mL solution of P2 (1×10^{-5} M) in ethanol was added to 1 equiv. of series of cations like Ca^{2+}, Cr^{2+}, Fe^{2+}, Fe^{3+}, Co^{2+}, Ni^{2+}, Cu^{2+}, Zn^{2+}, Cd^{2+}, Sn^{2+}, Hg^{2+}, and Pb^{2+}. Upon the addition of Cu^{2+} ions, the yellow-color solution of P2 changes to pink, while other competing cations did not show any intense and noticeable color change. However, a negligible color change was observed for Fe^{+2} and Fe^{+3}. This confirms that P2 could selectively detect Cu^{2+} ions with an intense color change over other cations (Fig. 1).

Continuing to support naked-eye sensing, UV–vis spectroscopic experiments were conducted. As depicted in UV–vis experiments, no absorbance was observed at 533 nm for all cations including P2 which demonstrates the closed form of the spirolactam ring present in P2. Further, adding 1 equiv. Cu^{2+} ions into P2 solution, absorbance maxima were found at 533 nm which implies the charge transfer from ligand to metal leading to the formation of coordination bond [27]. As shown in Fig. 1, though colorimetric changes were observed in the case of Fe^{2+} and Fe^{3+}, in UV–vis spectra it was indicated that P2 showed maximum absorbance at 533 nm only in presence of Cu^{2+} ions. Whereas other cations such as Ca^{2+}, Cr^{2+}, Fe^{2+}, Fe^{3+}, Co^{2+}, Ni^{2+}, Zn^{2+}, Cd^{2+}, Sn^{2+}, Hg^{2+}, and Pb^{2+} did not show spectral alterations (Fig. 2a).

3.2. UV–vis titration, interfering ions, and pH and time-dependent observations of P2

Further, to evaluate the complex forming mechanism and sensing ability of P2 with Cu^{2+} ions, UV–vis titrimetric experiments were performed with the incremental addition of Cu^{2+} ions (0–3 equiv.) to P2 (1×10^{-5} M). The peak centered at 460 nm in UV–vis spectra corresponds to the –OH functionality of P2. The incremental addition of Cu^{2+} ions to P2 resulted in gradual decreases in the absorption peak at 427 nm with a concurrent increase of a new peak at 533 nm forming an isosbestic point at 485 nm. This gradual decrease in absorption and generation of a new absorption peak suggests the involvement of the –OH functional group in the detection procedure. The increase in the absorbance intensity at 533 nm with a bathochromic shift of 73 nm is ascribed to the charge transfer transitions from ligand to Cu^{2+} that cause complex formation between P2 and Cu^{2+} with a significant change in color from yellow to pink. Furthermore, upon the addition of Cu^{2+} (0.2 equiv. to 3 equiv.) the increase in the intensity at 533 nm reached saturation after the addition of 3 equiv. of Cu^{2+} which suggested P2 is highly specific towards Cu^{2+} ions (Fig. S9c). In addition, the stoichiometric complexation between P2 and Cu^{2+} was studied using Job's method (Fig. 2b inset).

Further, the B–H (Benesi-Hildebrand) technique was used to calculate the binding stoichiometry of P2 and Cu^{2+} ions. By plotting $1/(A-A_0)$ vs. $1/[Cu^{2+}]$ (Fig. S10a) it was clear that P2 and Cu^{2+} ions had a 1:1 stoichiometric complexation. Then, using formula $3 \times \sigma/k$ (where σ: standard deviation, k: the slope of the calibration plot), the LoD (limit of detection) for Cu^{2+} in aqueous media was calculated to be 9.633×10^{-8} M (0.006 ppm) (Fig. S10b). The results showed that LoD is significantly lower than the EPA's allowed limit for Cu2+ ions.

Moreover, P2 was also examined for the influence of other cations during Cu^{2+} ion detection (Fig. 3a). To analyze this, 1 equiv. of each cation was added to a P2 solution (1×10^{-5} M in ethanol). UV–vis spectra of each metal ion-induced P2 solution was recorded wherein the spectral variation was observed only in presence of Cu^{2+} and Ni^{2+} ions. But the absorbance observed for Ni^{2+} was negligible in comparison with Cu^{2+}. Later, 1 equiv. Cu^{2+} ions were introduced to the above series of solutions (P2+metal ions) and were subjected to UV–vis spectral studies. It was noted that after adding Cu^{2+} ions into the P2 solution containing other cations, the intensity of metal at 533 nm was increased substantially which indicated that the detection of Cu^{2+} ions is possible even in presence of other cations (Fig. 2a).

Additionally, studies regarding the stability of P2 molecules at various pH are of high importance to use them as receptors in real-

Fig. 1. The color change of (a) P2 (1×10^{-5} M) in ethanol upon introducing 1 equiv. of various cations, (b) Ca^{2+}, (c) Cr^{2+}, (d) Fe^{2+}, (e) Fe^{3+}, (f) Co^{2+}, (g) Ni^{2+}, (h) Cu^{2+}, (i) Zn^{2+}, (j) Cd^{2+}, (k) Sn^{2+}, (l) Hg^{2+}, and (m) Pb^{2+}.
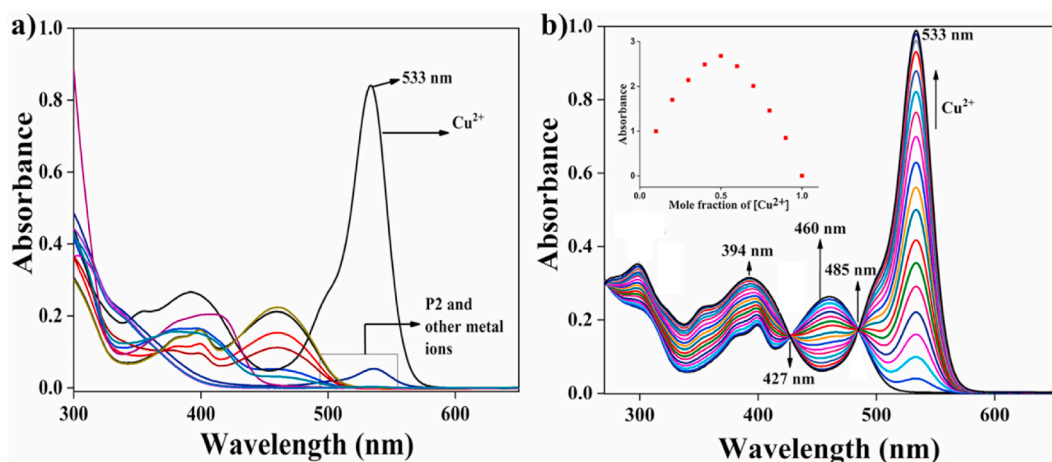
Fig. 2. (a) UV–vis spectral differences of receptor P2 (1×10^{-5} M in EtOH) with different cations (Ca^{2+}, Cr^{2+}, Fe^{2+}, Fe^{3+}, Co^{2+}, Ni^{2+}, Cu^{2+}, Zn^{2+}, Cd^{2+}, Sn^{2+}, Hg^{2+}, and Pb^{2+}). (b) UV–vis titration spectrum of P2 (1×10^{-5} M in ethanol) with the progressive addition of Cu^{2+} ions. Inset: Job's graph representing 1:1 stoichiometric complexation of P2 and Cu^{2+}.
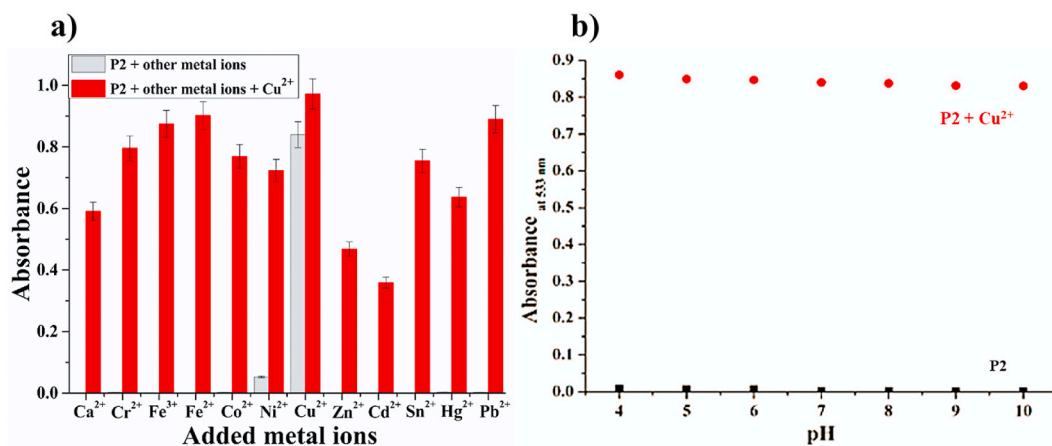
Fig. 3. (a) Absorbance enhancement factor of P2 for Cu^{2+} ions in the existence of competing cations. (b) The change in the absorbance of P2 (1×10^{-5} M) at various pH ranges (pH 4 - pH 10) in the presence or absence of 1 equiv. Cu^{2+} ions.

time applications. To recognize optimal pH conditions for real-time applications, the absorbance of P2 was recorded by including and excluding the Cu^{2+} ions at varied pH (i.e., from pH 4 to pH 10). As shown in Fig. 3b, it is noticed that, when the P2 solution was in an acidic condition (from pH 4 to pH 6), the intensity of absorbance was increased as it undergoes structural alteration due to the presence of rhodamine moiety which is sensitive at acidic pH. The drop in absorbance values was found in alkaline conditions, i.e., pH > 7.0 to 10, which is caused by CuO involvement in the detection process. Thus, it was confirmed that P2 is stable at both acidic and basic pH. Hence pH studies revealed that P2 is a potential organic probe to use in practical applications. However, pH 7 was considered for all the experiments as it is the general pH of water. Moreover, time studies were also performed to study the stability of the receptor molecule over time. 1 equiv. of Cu^{2+} ions was added to the receptor (1×10^{-5} M) and UV spectra are observed for every single hour, it is noticed that there is no variation in the color (remains pink) even after 24 h of time gap (Fig. S11). Moreover, to analyze the effect of the geometry of receptor P2 before and after interaction with Cu^{2+} ions, optimization of the re3ceptor P2 and the complex formed was carried out employing the Gaussian 09 program, which indicated that the xanthene moiety and isoindoline-1-one moiety of receptor P2 are perpendicular to each other and remain same even after complexation with Cu^{2+}, hence it is clear that there is no change in the geometry of the receptor upon complexation (Fig. S2).

3.3. Copper detection mechanism

Upon the addition of Cu^{2+} ions, the receptor will form a coordination bond with Cu^{2+} which affords to change in color. The co-ordination complex formation between Cu^{2+} ions and P2 is due to the ligand-to-metal charge transfer (LMCT) that induces a considerable color change from yellow to pink. Scheme S2 represents a possible detection mechanism. However, the prepared

rhodamine derivative consists of a strong electron-withdrawing group –NO_2, which results in a closed spirolactum ring even after the addition of Cu^{2+} ions. Thus, the fluorescence properties of typical rhodamine structure after treatment with Cu^{2+} ions vanished [27] Hence, it was evidence that P2 could show the color change that can be observed through the naked eye.

3.4. Characterization of functionalized diatom (P2D)

Analytical methods including FESEM, EDAX, and BET were used to confirm the functionalization of P2 on DE. FESEM analysis was performed to understand the morphological variations before and after the functionalization with P2. Fig. 4a shows the cylindrical morphology of the bare DE frustules where the uniform distribution of nanopores of the DE is visible. After treatment with P2, a thick layer formation was observed which was due to the tethering of organic molecules on the surface (Fig. 4b). The immobilization of P2 partially or completely covered the nanopores on the DE surface. Further, to confirm the decoration of P2 on the DE surface, elemental analysis was performed (Fig. S12), which confirmed that P2D displays peaks for Si, O, C, and N which indicated that the P2 is functionalized on DE as displayed in Scheme 1.

Besides, BET surface analysis was carried out on bare DE and P2D microparticles to examine the influence of surface modifications on the surface area after the decoration with P2. The liquid N_2 temperature with 1 bar pressure was used to measure adsorption isotherms. Before the measurement, the samples were preheated at 100 °C under vacuum for 2 h to remove the interlayer moisture. As shown in Table 1, the surface area and pore volume of bare diatoms (21.10 m^2/g; 0.023 cm^3/g) were reduced upon modification with the P2 molecule (10.524 m^2/g; 0.018 cm^3/g). The decrease in the surface area after immobilizing P2 was thought to be a cause of the existence of an organic layer on the DE surface that closed the maximum nanopores present on bare DE. This observation was well evidenced by FESEM analysis. The adsorption-desorption isotherm of bare DE and P2D microparticles were shown in Fig. S13. The isotherm plots which demonstrate the porous nature of DE before and after modification allow us to classify them as standard type II isotherms due to the presence of a modest hysteresis loop. Thus, these analytical techniques proved that P2 had been successfully immobilized on DE employing APTES as an intermediate.

3.5. Removal of copper ion and fabrication of a device employing P2D

From the above studies, it was clear that P2 is highly selective towards Cu^{2+} ions over the other competing cations, as it forms a coordination complex with the Cu^{2+} ions. Considering this interaction, an effective adsorbent was developed by decorating the P2 molecule on the surface of the DE. Later, to understand the removal efficiency of the P2D molecule, 1 mL Cu^{2+} (1 ppm) was added to the 50 mg of P2D. The above solution was sonicated for 2 min and centrifuged to yield the clear supernatant solution. This supernatant solution was further treated with P2. The UV–vis spectra of the above solution were recorded to recognize trace amounts of Cu^{2+} ions. Interestingly there was no absorbance peak found at 533 nm which implies that there was no trace of Cu^{2+} ions supernatant solution. The procedure was repeated and after the 11th addition, the absorbance peak at 533 nm emerged which indicates the presence of free Cu^{2+} in the supernatant solution (Fig. 5a) which indicates the limit of P2D to bind with Cu^{2+} ions. Additionally, the reproducibility studies were carried out for 5 cycles (n = 5) and the standard deviation calculated is 1.5.

Furthermore, a cartridge has been devised for the removal of Cu^{2+} ions from water [30]. Though the results were prominent, the removal process has a limitation which was the batch mode removal of Cu^{2+} ions. To overcome this, a device has been designed which can be used to remove Cu^{2+} ions continuously. As displayed in Fig. 5b, the device consists of an inlet, an outlet, and a place for packing material. The device has been placed upright and P2D material was filled into the device. The loss of P2D material through the removal process was stopped by keeping the small cotton bed before filling the material. The device was fixed to a conical flask containing a vacuum inlet. The removal process was initiated by keeping the inlet in the copper-rich water sample and applying the vacuum which helps to suck the solution to feed it to the P2D and copper-free water will be collected through the outlet provided. This process will help in the continuous removal of Cu^{2+} ions from water. Apart from this, real samples studies were also carried out for various matrices such as agricultural waste, and pharmaceutical effluent. The solution (diluted 20 times) of these matrices was added to the receptor (1
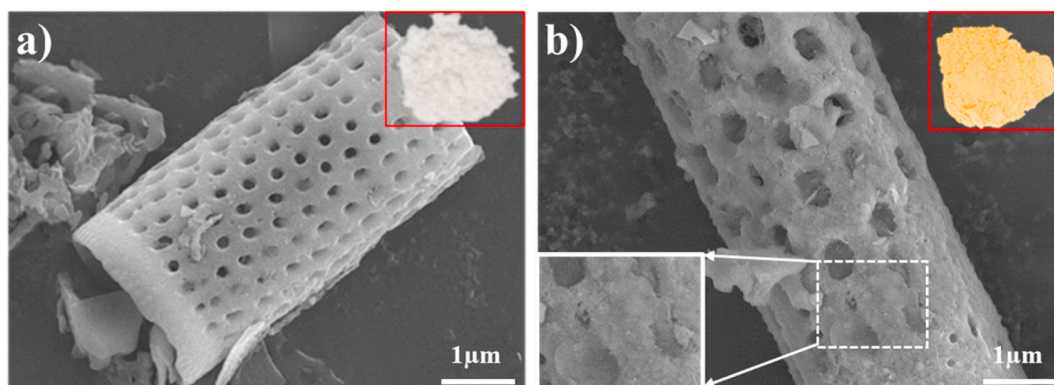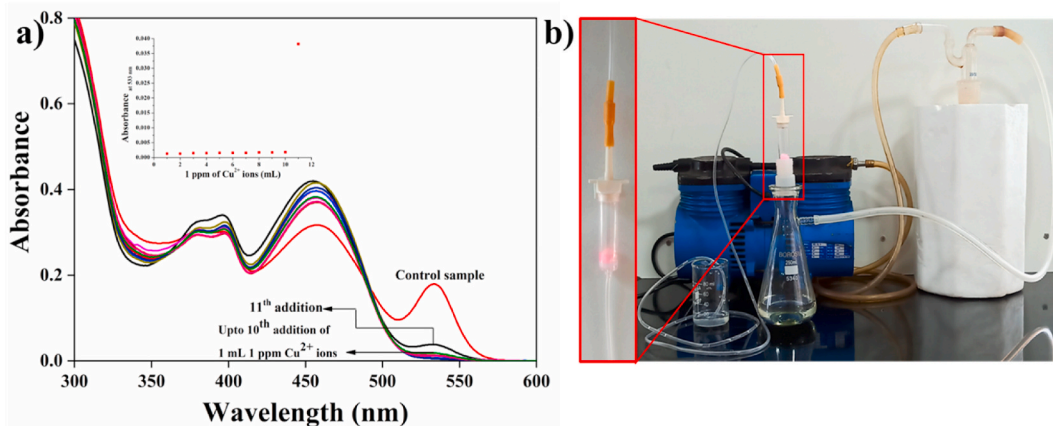

Fig. 4. FESEM images of (a) bare DE, (b) P2 functionalized DE (P2D), inset: change in the color of P2D after surface modification with P2.

Table 1
BET surface area analysis data of bare DE and P2D.

Sample	Surface area (m²/g)	Pore Volume (cm³/g)
Bare DE	21.10	0.0233
P2D	10.524	0.0182

Fig. 5. (a) UV–vis absorbance spectra of 1 ppm Cu^{2+} removal incorporating P2D. (b) Real-time pictures of the device design for Cu^{2+} ions removal from water using P2D.

$\times 10^{-5}$ M). which resulted in color changes from yellow to pale pink, and yellow to pink for agricultural and pharmaceutical waste respectively (Fig. S9b) which were also evident by UV visible spectra (Fig. S9d). Further the amount of copper present in the real-time samples (agricultural wastewater, and pharmaceutical waste) was calculated using a calibration curve, which is found to be 0.031×10^{-6} M(0.001 ppm), 0.068×10^{-6} M (0.004 ppm) (Fig. S14). Furthermore, an effort has been made to compare the efficiency of developed technology and other reported simultaneous Cu^{2+} detection and removal techniques. The LoD, removal efficiency of Cu^{2+} using various types of materials, and their detection methods are compiled in Table 2.

4. Conclusions

A highly selective rhodamine derivative (P2) bearing 2-hydroxy 5-nitrobenzaldehyde was successfully synthesized and characterized for its structural confirmation. P2 can be used to selectively detect Cu^{2+} ions in context with other competing ions. The yellow color of P2 in ethanol turned pink only upon the addition of Cu^{2+} ions whereas other competing ions did not show any considerable color change. The P2 showed excellent anti-interference properties for other metal ions with a 9.663×10^{-8} M (0.006 ppm) limit of detection and also stable over pH values ranging from 4 to 10. The UV–vis titration studies revealed a stoichiometric complexation of a 1:1 ratio that occurs between P2 and Cu^{2+} ions. Further, P2 was effectively immobilized on naturally occurring DE which was further confirmed using analytical techniques such as FESEM, EDAX, and BET. Besides, P2D was also investigated for the removal of Cu^{2+} ions where results showed that 50 mg of functionalized DE (P2D) was capable to remove 10 mL of Cu^{2+} ions from water. In addition to this, an easy-to-use device has been developed for the continuous removal of Cu^{2+} ions with $\leq 99.9\%$ efficiency. These kinds of devices can be utilized in remote areas and the industries for efficient removal of Cu^{2+} ions where the efficiency of material can be observed through the naked eye.

Author contribution statement

Padmaja V Mane: Performed the experiments; Analyzed and interpreted the data; Wrote the paper.
Pravin Patil: Performed the experiments.
Anusha A. Mahishi: Analyzed and interpreted the data.
Madhuprasad Kigga: Conceptualization; supervision
Mahesh P Bhat: Conceived and designed the experiments; editing; supervision
Kyeong-Hwan Lee; Mahaveer D. Kurkuri: Resources; supervision; contributed reagents, materials, analysis tools or data.

Data availability statement

Data will be made available on request.

Table 2
Comparison of prior studies for the simultaneous detection and removal of Cu^{2+} with the current study.

Sensor	Method	Detection limit	Removal efficiency (%)/Adsorption capacity (mg/g)	Reference
phenazine (AHPN)	UV–visible spectra	1×10^{-6} M	76%	[31]
naphthalimide-based GO–cellulose membrane	Fluorescence method	7.3×10^{-7} M	96%	[32]
Composite adsorbent	Colorimetric method	0.0015×10^{-6} M	200.80	[33]
(p (HEMA-co-TACYC))	Colorimetric method	0.0370×10^{-6} M	–	[34]
composite material (MeCM)	optical method	0.0015×10^{-6} M	197.15	[35]
Hydrogels Composite material	optical method	0.0039×10^{-6} M	171.33	[36]
spherical magnetic nanocomposite (SDMA)	Fluorescence method	0.7937×10^{-6} M	80% of Cu^{2+} from 10 mL	[37]
Europium (III) complex-functionalized magnetic nanoparticle	Fluorescence method	0.1×10^{-9} M	70%	[38]
diamine-functionalized SBA-15	Colorimetric method	0.0152×10^{-3} M	27.22	[39]
Rhodamine-6G	Colorimetric method	9.6330×10^{-8} M (0.006 ppm)	≤99.9% of Cu^{2+} from 11 mL	This work

Declaration of competing interest

Acknowledgment

Appendix A. Supplementary data

Supplementary data to this article can be found online at https://doi.org/10.1016/j.heliyon.2023.e16600.

References

[1] A. Bilgic, A. Cimen, A.N. Kursunlu, "Killing two birds with one stone": a fluorescent hybrid nanoparticle modified with BODIPY for efficiently detection and removal of toxic Cu (II) ion from aqueous solutions, Sci. Total Environ. 845 (2022), 157170.

[2] A. Kumar, A. Kumar, M. Dubey, A. Biswas, D.S. Pandey, Detection of copper(ii) and aluminium(iii) by a new bis-benzimidazole Schiff base in aqueous media via distinct routes, RSC Adv. 5 (108) (2015) 88612–88624.

[3] H.-j. Yu, W. Zhao, Y. Zhou, G.-j. Cheng, M. Sun, L. Wang, L. Yu, S.H. Liang, C. Ran, Salen-based bifunctional chemosensor for copper (II) ions: inhibition of copper-induced amyloid-β aggregation, Anal. Chim. Acta 1097 (2020) 144–152.

[4] Y.-D. Xia, Y.-Q. Sun, Y. Cheng, Y. Xia, X.-B. Yin, Rational design of dual-ligand Eu-MOF for ratiometric fluorescence sensing Cu2+ ions in human serum to diagnose Wilson's disease, Anal. Chim. Acta 1204 (2022), 339731.

[5] C.A.S. Pothulapadu, A. Jayaraj, R.N. Priyanka, G.J.Ao. Sivaraman, Novel benzothiazole-based highly selective ratiometric fluorescent turn-on sensors for Zn2+ and colorimetric chemosensors for Zn2+, Cu2+, and Ni2+ ions, ACS Omega 6 (38) (2021) 24473–24483.

[6] X. Qiao, G. Chen, T. Yue, Q.J.o.A.C. Sheng, A functional fluorescent probe for Zn2+ and Cu2+ detection in Food products based on tetraphenylethylene derivative, J. Anal. Chem. 77 (9) (2022) 1131–1140.

[7] Y. Li, F. Lu, Q.-z. Li, Y.-h. Zhou, J. Qian, S. Cao, C.-y.J.R.a. Wang, An ink-jet printed dual-CD ratiometric fluorescent paper-based sensor for the visual detection of Cu 2+, RSC Adv. 11 (52) (2021) 33036–33047.

[8] P.A.I. Fernando, E. Alberts, M.W. Glasscott, A. Netchaev, J.D. Ray, K. Conley, R. Patel, J. Fury, D. Henderson, L.C.J.A.o. Moores, In situ preconcentration and quantification of Cu2+ via chelating polymer-wrapped multiwalled carbon nanotubes, ACS Omega 6 (8) (2021) 5158–5165.

[9] H. Sharifi, J. Tashkhourian, B. Hemmateenejad, A 3D origami paper-based analytical device combined with PVC membrane for colorimetric assay of heavy metal ions: application to determination of Cu(II) in water samples, Anal. Chim. Acta 1126 (2020) 114–123.

[10] M. Samadifar, Y. Yamini, M.M. Khataei, A.J.S.S.P. Badiei, Ethylenediaminetetraacetate functionalized ordered Santa Barbara Amorphous-15 mesoporous silica as an effective adsorbent for preconcentration of some heavy metals followed by inductively coupled plasma atomic emission spectrometry, Seperation Sci. Plus 5 (3–4) (2022) 75–83.

[11] H.-J. Hwang, G.-H. Hwang, S.-M. Ahn, S.-Y. Kim, H.-S.J.F. Shin, Risk assessment and determination of heavy metals in home meal replacement products by using inductively coupled plasma mass spectrometry and direct mercury analyzer, Foods 11 (4) (2022) 504.

[12] M.P. Bhat Madhuprasad, P. Patil, S.K. Nataraj, T. Altalhi, H.-Y. Jung, D. Losic, M.D. Kurkuri, Turmeric, naturally available colorimetric receptor for quantitative detection of fluoride and iron, Chem. Eng. J. 303 (2016) 14–21.

[13] X. Wang, S. Cheng, C. Liu, Y. Zhang, M. Su, X. Rong, H. Zhu, M. Yu, W. Sheng, B. Zhu, A novel ratiometric fluorescent probe for the detection of nickel ions in the environment and living organisms, Sci. Total Environ. 840 (2022), 156445.

[14] A. Hyder, J.A. Buledi, M. Nawaz, D.B. Rajpar, Y. Orooji, M.L. Yola, H. Karimi-Maleh, H. Lin, A.R.J.E.R. Solangi, Identification of heavy metal ions from aqueous environment through gold, Silver and Copper Nanoparticles: an excellent colorimetric approach, Environ. Res. 205 (2022), 112475.

[15] M.P. Bhat, M. Kurkuri, D. Losic, M. Kigga, T. Altalhi, New optofluidic based lab-on-a-chip device for the real-time fluoride analysis, Anal. Chim. Acta 1159 (2021), 338439.

[16] P. Patil, K.V. Ajeya, M.P. Bhat, G. Sriram, J. Yu, H.Y. Jung, T. Altalhi, M. Kigga, M.D.J.C. Kurkuri, Real-time probe for the efficient sensing of inorganic fluoride and copper ions in aqueous media, ChemistrySelect 3 (41) (2018) 11593–11600.

[17] K. Gupta, P. Joshi, R. Gusain, O.P.J.C.C.R. Khatri, Recent advances in adsorptive removal of heavy metal and metalloid ions by metal oxide-based nanomaterials, Coord. Chem. Rev. 445 (2021), 214100.

[18] A. Waheed, N. Baig, N. Ullah, W.J.J.o.E.M. Falath, Removal of hazardous dyes, toxic metal ions and organic pollutants from wastewater by using porous hyper-cross-linked polymeric materials: a review of recent advances, J. Environ. Manag. 287 (2021), 112360.

[19] W. Jing, J. Wang, B. Kuipers, W. Bi, D.D.Y.J.T.T.i.A.C. Chen, Recent applications of graphene and graphene-based materials as sorbents in trace analysis, TrAC, Trends Anal. Chem. 137 (2021), 116212.

[20] A. Saxena, A. Tiwari, R. Kaushik, H.M. Iqbal, R.J.J.o.W.P.E. Parra-Saldívar, Diatoms recovery from wastewater: overview from an ecological and economic perspective, J. Water Proc. Eng. 39 (2021), 101705.

[21] V. Panwar, T.J.A.A.B.M. Dutta, Diatom biogenic silica as a felicitous platform for biochemical engineering: expanding frontiers, ACS Appl. Bio Mater. 2 (6) (2019) 2295–2316.

[22] F. Zobi, Diatom biosilica in targeted drug delivery and biosensing applications: recent studies, Micro, MDPI (2022) 342–360.

[23] N.S. Sarai, B.J. Levin, J.M. Roberts, D.E. Katsoulis, F.H.J.A.C.S. Arnold, Biocatalytic transformations of silicon—the other group 14 element, ACS Cent. Sci. 7 (6) (2021) 944–953.

[24] V. Zeni, G.V. Baliota, G. Benelli, A. Canale, C.G.J.M. Athanassiou, Diatomaceous earth for arthropod pest control: back to the future, Molecules 26 (24) (2021) 7487.

[25] N. Rabiee, M. Khatami, G. Jamalipour Soufi, Y. Fatahi, S. Iravani, R.S.J.A.b.s. Varma, engineering, Diatoms with invaluable applications in nanotechnology, biotechnology, and biomedicine: recent advances, ACS Biomater. Sci. Eng. 7 (7) (2021) 3053–3068.

[26] P. Aggrey, M. Nartey, Y. Kan, J. Cvjetinovic, A. Andrews, A.I. Salimon, K.I. Dragnevski, A.M.J.R.a. Korsunsky, On the diatomite-based nanostructure-preserving material synthesis for energy applications, RSC Adv. 11 (51) (2021) 31884–31922.

[27] M.P. Bhat, M. Kigga, H. Govindappa, P. Patil, H.-Y. Jung, J. Yu, M.J.N.J.o.C. Kurkuri, A reversible fluoride chemosensor for the development of multi-input molecular logic gates, New J. Chem. 43 (32) (2019) 12734–12743.

[28] P. Patil Madhuprasad, M.P. Bhat, M.G. Gatti, S. Kabiri, T. Altalhi, H.-Y. Jung, D. Losic, M. Kurkuri, Chemodosimeter functionalized diatomaceous earth particles for visual detection and removal of trace mercury ions from water, Chem. Eng. J. 327 (2017) 725–733.

[29] Y. Ding, W. Zhu, Y. Xu, X. Qian, A small molecular fluorescent sensor functionalized silica microsphere for detection and removal of mercury, cadmium, and lead ions in aqueous solutions, Sensor. Actuator. B Chem. 220 (2015) 762–771.

[30] Shrinath Bhat, U.T. Uthappa, T. Sadhasivam, Altalhi Tariq, Soo Han Sung, Mahaveer D. Kurkuri, Abundant cilantro derived high surface area activated carbon (AC) for superior adsorption performances of cationic/anionic dyes and supercapacitor application, Chem. Eng. J. 459 (2023), 141577.

[31] Tai-Bao Wei, Yong Bi-Rong, Li-Rong Dang, You-Ming Zhang, Hong Yao, Lin Qi, A simple water-soluble phenazine dye for colorimetric/fluorogenic dual-mode detection and removal of Cu2+ in natural water and plant samples, Dyes Pigments 171 (2019), 107707.

[32] Meng Li, Zhijiang Liu, Shuwen Wang, David G. Calatayud, Wei-Hong Zhu, Tony D. James, Lidong Wang, Boyang Mao, Hui-Ning Xiao, Fluorescence detection and removal of copper from water using a biobased and biodegradable 2D soft material, Chem. Commun. 54 (2) (2018) 184–187.

[33] Md Rabiul Awual, Md Munjur Hasan, Colorimetric detection and removal of copper (II) ions from wastewater samples using tailor-made composite adsorbent, Sensor. Actuator. B Chem. 206 (2015) 692–700.

[34] Asadollah Beiraghi, Najibi-Gehraz Seyed Ali, Carbon dots-modified silver nanoparticles as a new colorimetric sensor for selective determination of cupric ions, Sensor. Actuator. B Chem. 253 (2017) 342–351.

[35] Md Rabiul Awual, Md Munjur Hasan, Mohammed M. Rahman, Abdullah M. Asiri, Novel composite material for selective copper (II) detection and removal from aqueous media, J. Mol. Liq. 283 (2019) 772–780.

[36] Md Rabiul Awual, Novel ligand functionalized composite material for efficient copper (II) capturing from wastewater sample, Compos. B Eng. 172 (2019) 387–396.

[37] Xun Qiu, Najun Li, Shun Yang, Dongyun Chen, Qingfeng Xu, Hua Li, Jianmei Lu, A new magnetic nanocomposite for selective detection and removal of trace copper ions from water, J. Mater. Chem. 3 (3) (2015) 1265–1271.

[38] Jing Liu, Wei Zuo, Wei Zhang, Jian Liu, Zhiyi Wang, Zhengyin Yang, Baodui Wang, Europium (III) complex-functionalized magnetic nanoparticle as a chemosensor for ultrasensitive detection and removal of copper (II) from aqueous solution, Nanoscale 6 (19) (2014) 11473–11478.

[39] Zhuqing Wang, Min Wang, Genhua Wu, Dayu Wu, Aiguo Wu, Colorimetric detection of copper and efficient removal of heavy metal ions from water by diamine-functionalized SBA-15, Dalton Trans. 43 (22) (2014) 8461–8468.